Sci. J. Fac. Sci., Minufiya Univ., Vol. XVII (2003 : 261 – 308)

GENESIS OF BISMUTH AND BERYLLIUM MINERALIZATION AT WADI GHAZALA AREA (SE SINAI, EGYPT) : CRITERIA FROM THE MINERAL CHEMISTRY AND FLUID INCLUSIONS

Adel A. Surour

Department of Geology, Faculty of Science, Cairo University, Giza, Egypt

Received 1 / 2 / 2003

Abstract

The present study uses the tools of mineral chemistry and fluid inclusions in order to characterize the beryl of Wadi Ghazala occurrence. Recently, some workers (Abdalla et al., 2001) believed that the beryl crystallized in pegmatitic leucosomes resulting from migmatization. Field observations of the present author suggest the presence of a small-scale shear zone along which beryl-bearing pegmatites and quartz veins invade an amphibolite country rock. At the outcrop, the amphibolite shows gradual transformation into a dark mica rock indicating K-metasomatism which is also documented petrographically. This observation, combined with the presence of some mica inclusions in the beryl, is not in favour of crystallization by metamorphic segregation. In addition to beryl, the pegmatites of Wadi Ghazala also contain other typical hydrothermal minerals such as

fluorite, columbite and bismuth minerals. The latter are represented by bismuthinite, bismite and beyerite. Mineral chemistry of beryl and the dark micas shows characteristics of hydrothermal systems. Such conclusion is also supported by the homogenization temperatures of primary and secondary fluid inclusions in the beryl that suggest trapping of hydrothermal fluids at 174-265 °C. Salinity of the fluid inclusions is peculiar (as low as 1.37 wt% $NaCl_{eq}$) in comparison with the other world examples indicating high degrees of mixing with meteoric waters within the shear zone which also resulted in the disappearance of any daughter crystals in the investigated inclusions.

Keywords

beryl- dark micas- fluid inclusions- hydrothermal- migmatization

Introduction

Very little have been published on the occurrence of beryl in the Sinai Peninsula, which is in fact known as a province of another gemstone "turquoise" since the time of the Ancient Egyptians. Discovery of beryl mineralization in Sinai is only dated back to the last decade. El-Aassy et al. (1993) presented the first description of beryl from Sinai at Wadi Ghazala, and distinguished two mineral varieties; white to grey beryl and green emerald. El-Aassy et al. (1993) and Hamad (1995) came to the conclusion that the beryl associates mica and actinolite schists that might represent allochtonous serpentinite

pockets. It seems that these authors are inclined to consider the beryl mineralization at the occurrence of Wadi Ghazala as an analogue to the "schist-type" beryl deposits in the Eastern Desert of Egypt. In general, the beryl deposits in the Eastern Desert are classified into: a) disseminated ore in some specialized granites, and b) "schist-type" deposits along the contact between the ophiolitic ultramafic rocks and within-plate intrusive granites (Hassan and El-Shatoury 1976; El-Dougdoug et al. 1997; Omar 2001, Takla et al., 2002).

Recently, Abdalla et al. (2001) published the third and time wise the last paper on the beryl mineralization at the occurrence of Wadi Ghazala in Sinai. Confinement of the beryl-bearing veins to some gneissose rocks led Abdalla et al. (2001) to establish a genetic model based on migmatization at amphibolite facies conditions. The authors believed that beryl is encountered in quartz and K-feldspar leucosomes that are commonly interlayered with phlogopite melanosomes. They also discarded any model in favour of metasomatism along igneous pegmatites and stated clearly that the beryl-bearing leucosomes represent abyssal metamorphic pegmatites that were formed at 650-700 °C and 5-7 kbar. Nevertheless, Abdalla et al. (2001) did not present any geothermometric calculations of the metamorphic assemblages in equilibrium or fluid inclusions microthermometric measurements to support the suggested temperature and pressure.

The purpose of the present study is the characterization of the beryl mineralization at Wadi Ghazala occurrence on the basis of combined criteria from the field observations, microscopic-scale textures, mineral chemistry and fluid inclusions data. In this respect, the first information about the conditions of beryl formation are obtained from the microthermometric measurements of the trapped fluid inclusions, which has its direct implication on the genesis of the beryl in consideration. In other words, the paper aims directly to justify and fit a reasonable genetic model in the context of the origin of the pegmatite host (igneous or metamorphic?). The paper also presents the first electron microprobe analyses of Wadi Ghazala beryl and the associated minerals that can be used for the accurate determination of mineral composition and the evolutionary history of the host rocks. Of course, mineral chemistry of the assemblages in the host rocks can demonstrate whether these rocks have suffered high-grade anatexis or not. The paper presents the first mineralogical account for bismuth mineralization in Sinai. Such account concerns with the identification of the recorded bismuth minerals, their chemical composition and its implications on the genesis of beryl.

Field Observations

At the studied occurrence of Wadi Ghazala, the beryliferous zones are very few in number and their extension at the outcrops is limited, never exceeding 250 m in length and 10-15 m in width. The principal beryliferous zone is recorded in porphyritic syenogranite (Fig. 1). The seynogranite shows local gneissosity at the borders of the beryliferous zone. It appears that the outcrops represent uplifted fragments along a series of NNE-SSW faults. Uplifting of the beryliferous zones is documented by the presence of consolidated wadi deposits that unconformably overlie the beryliferous zone. These wadi deposits are composed of multi-component gneisses and granitic pebbles and coubles set in a fine carbonate clayey matrix.

Generally, it appears that faulting was responsible for the development of a local shear zone along which the beryl-bearing bodies are confined. At the same time, the country rocks (syenogranite with unmappable amphibolite bodies) were also deformed. Existence of such a shear zone is supported by the absence of shearing or any gneissose texture in the country rocks on getting away from the beryliferous zones. Outside this zone, the syenogranite as well as another type of within-plate granites (monzogranite), display distinct porphyritic texture and interlocking fabrics.

Field anatomy of the beryliferous zone revealed that it is composed of the following members: a) beryl-bearing quartz veins, b) beryl-bearing pegmatites, and c) amphibolite. The amphibolite is massive but it shows local schistose-like appearance due to shearing especially along the contact with the pegmatites. Field observations show that both the quartz and pegmatite veins invade the amphibolite and in some instances small-scattered quartz and pegmatite boudins are seen infiltrating the amphibolite. It is evident that the amphibolite is partly transformed into a contorted dark mica rock along the contact with the felsic veins and boudins. Such observation, which is also documented microscopically, suggests that the felsic bodies were introduced to the amphibolite as injections. Occurrence of sub-parallel beryl-bearing quartz veins traversing the pegmatites is also another evidence of the injection hypothesis. Accordingly, the contorted dark mica rock can not represent melanosomes produced by anatexis as suggested by Abdalla et al. (2001). Formation of the mica rock at the expense of the amphibolite is based not only on field aspects but also on some criteria from the mineral chemistry and fluid inclusions as well.

In contrast to the previous studies that describe beryl at Wadi Ghazala as small-scattered crystals in the felsic veins, the present author was able to record large boudins (15 cm x 25 cm) composed of aggregated beryl crystals that are nearly free of quartz. These boudins are lensoidal in shape and selvaged by dense mica sheaths. Beryl in these boudins is coarse, undeformed and exhibits bluish green colour. Sometimes, the crystals are rough and dull which is attributed to natural chemical etching processes (Bowersox et al. 1991). The beryl of Wadi Ghazala also associates bismuth mineralization, commonly in the form of canary-yellow bismuth gossans. A detailed mineralogical study on the bismuth mineralization in the vicinity of the beryliferous zones at Wadi Ghazala is given in the present paper in a later section .

Mineral Assemblages and Textures

As previously shown in the section on field observations, there are different beryl-bearing rock varieties within the beryliferous zone of Wadi Ghazala. In this section, the petrographic characteristics of all varieties are given in order to specify their mineral assemblages and textures. Also, short accounts on the paragenesis of the country rocks (amphibolites and granites) are given. In agreement with the preliminary identification at the outcrops, the rock varieties in the beryliferous zone are classified into beryl-bearing quartz and pegmatite veins and dark mica rocks. In the following, the results of the microscopic investigation are presented in which both types of

veins are lumped together because of their similar ore paragenesis that is represented by beryl (I & II) and fluorite. The sole difference is that some of the pegmatites bear bismuth minerals and columbite

Beryl-bearing quartz and pegmatite veins:

In both varieties, beryl occurs as subhedral to euhedral six-sided prismatic crystals. Beryl in the quartz veins is more euhedral and contains rare mica or quartz inclusions. On the other hand, beryl in the pegmatites is mostly subhedral and encloses several inclusions. It is evident that two generations of beryl are recorded; in which a coarse subhedral generation captures another smaller generation in the form of vug filling. The second generation occurs as euhedral fine crystals with parting and associates interstitial bismuth minerals in the vugs (Fig. 2a). In terms of abundance, the earlier generation represents around 95 % of the beryl minerals. It is preferentially corroded by quartz and K-feldspars, but the beryl itself corrodes the mica flakes and takes some of them as inclusions, particularly at the peripheral zones (Fig. 2b). The presence of the micas inclusions (mostly phlogopite) in Wadi Ghazala beryl excludes their formation by metamorphic segregation as melanosomes.

The paragenetic sequence shows that fluorite is clearly younger than beryl and the latter is often invaded or encrusted by the former. Along cracks in the beryl, fluorite is more or less mosaiced in a comb-

strucured pattern and associates microcrystalline quartz. In the groundmass, fluorite is massive and incorporates inclusions of oriented mica flakes. Some of the beryl-bearing pegmatite veins also contain discrete crystals of accessory columbite. Identification of columbite was verified by the EDS spectra during the work on the electron microprobe.

Metasomatized amphibolite and dark mica rock:

The investigated amphibolite is either massive or sheared depending on the position of sampling with respect to the shear zone. In all cases, the amphibolite is melanocratic owing to its high content of dark amphiboles whereas plagioclase amounts to 3-5 % only. Compositionally, the ampiboles range from actinolitic hornblende to hornblende. The hornblende is green and occurs as prismatic and rhombic cross-sectional crystals. Careful microscopic investigation allows the detection of hornblende replacement by dark brown micas (Fig. 2c). The degree of replacement becomes more extensive near the contact with the pegmatites indicating a pervasive event of K-metasomatism. Abdalla et al. (2001) did not record such type of replacement and hence they were inclined to an anatectic origin of both the micas and the beryl. Plagioclase in the studied amphibolites is anhedral due to growth of amphibole, and the former contains frequent needle-like inclusions of apatite. Some samples of the amphibolite also

contain rutile, which in turn represents an alteration of frequent ilmenite (5-7 %). The ilmenite also shows rim replacement by titanite in the form of atoll structure.

Mineralogically, the dark mica rocks are composed mainly of micas (>95 %) that range in composition from phlogopite to biotite. The mica rocks also contain some amphibole relics, in addition to quartz, magnetite, zircon and apatite. The mica flakes are almost fresh and exhibit interlocked fabrics. They are characterized by the presence of numerous inclusions of metamict zircon (Fig. 2d). Magnetite in the mica rocks is always euhedral and shows cross-cutting relations with the silicates indicating its introduction to the rock during the event of metasomatism. This assumption is also supported by the fact that some fine magnetite octahedra are preferentially arranged along the boundaries between the amphibole relics and the growing amphiboles.

Monzo- and syenogranites:

Both varieties of the granites contain porphyritic crystals of microcline perthite and much lesser homogeneous orthoclase or orthoclase perthite. As a result of shearing, biotite in many granitic samples is highly squeezed and shows partial alteration to chlorite (pennine). Plagioclase is mostly fresh and shows infiltration by quartz

and apatite. The main accessories in the granites are homogeneous magnetite and zoned zircon. In addition to its presence in the pegmatites, columbite with some features of metamictization is also recorded in the granitic country rock (Fig. 3a).

Analytical Methods

The electron microprobe analyses of Wadi Ghazala beryl and other associated minerals were carried out in Denmark at the University of Copenhagen using a JEOL superprobe 733 equipped with four wavelength-dispersive spectrometers. Operating conditions were 15 kV acceleration voltage, 15 nA beam current and a beam diameter of 1-3 μm. A set of natural and synthetic standards (silicates and oxides) was used for calibration and the measuring time of all elements was constant (20 seconds). The obtained analytical data were then reduced and corrected using a ZAF routine program. Under the described conditions, the analytical error was ±1 relative to nine of the major elements and 5% relative to both Ni and Cr.

The study of fluid inclusions was achieved at the Department of Geology, Cairo University using a USGS freezing-heating stage. Measurements were based on a 2 mm thick doubly-polished wafers of beryl. The accuracy of phase transation temperature measurements was in the range of ±0.5 °C to ±2 °C. Because the temperature of final

ice melting (T_i) is an expression of brine concentration (Bodnar and Vityk, 1994), the equivalent NaCl wt% was calculated using the equations cited in Potter and Brown (1977).

Mineral Chemistry

Beryl:

Table 1 gives the first electron microprobe analyses of beryl from Wadi Ghazala. Abdalla et al. (2001) presented some analyses of this beryl but they were based on solutions of digested crystals. Actually, the advantage of the beryl spot analyses by the microprobe is the complete elimination of chemical interference that is often caused by inclusions in the mineral. Data of Table 1 show analyses of spots at the cores as well as at the rims of independent beryl crystals. The table also contains analyses along two profiles in two representative crystals (beryl I & II) in order to follow if there is some chemical zoning since all crystals do not display optical zoning. It is evident that neither of the analysed generations of beryl display cryptic chemical zoning. The only valuable observation that can be obtained from the provided chemical profiles is the relative enrichment of Mg and alkalies at some rims.

The electron microprobe analyses of Wadi Ghazala beryl show that the ranges of Cr_2O_3, FeO, Mg and Na_2O are remarkably higher than the values previously reported by Abdalla et al. (2001) who

presented them as follows: 0.02-0.03 wt%, 0.16-0.41 wt%, 0.48-1.10 wt% and 0.51-0.78 wt%, respectively. According to the data of the present work, Na_2O lies in the range of 0.59-1.32 wt% which still classifies the beryl as sodic beryl (Hawthorne and Černý, 1977) similar to the beryl from the "schist-type" deposits of the Egyptian Eastern Desert (Takla et al., 2002). It is also worthy to mention that Cr_2O_3 content reaches up to 0.13 wt%, which is the same value of the oxide in the emerald of the Eastern Desert (El-Dougdoug et al. 1997). This amount of Cr traces is most probably the main cause of bluish green colouration of Wadi Ghazala beryl. In fact this statements does not necessarily mean the classification of some beryl crystals collected at the outcrops of Wadi Ghazala as emeralds. Of course, this needs more detailed investigations in terms of their gemmological characteristics.

In order to investigate the possible ionic substitutions in the structure of Wadi Ghazal beryl, some binary diagrams are constructed (Fig. 4). It is evident that the analysed beryl shows the same positive and negative substitutional trends that are displayed by the emeralds from the Eastern Desert, particularly those from the "schist-type" deposits along the contact between the ultramafic rocks and the granites. The only difference is the magnitude of ionic substitutions, which can be elucidated from either the oxide concentrations or the structural formulae. In this respect, the beryl of Wadi Ghazala contains relatively higher Al_2O_3 & FeO, and lower MgO & Na_2O than those in

the beryls from different occurrences in the Eastern Desert (Surour 1993; El-Dougdoug et al. 1997; Abdalla and Mohamed 1999; Omar 2001). On the basis of structural classification defined by Aurisicchio et al. (1988), the beryl of Wadi Ghazala has the affinity of the octahedral end-member because of substitutions in the octahedral sites. Figure 3 shows the different octahedral substitutions of Mg and Fe for Al in analogy to similar substitutions in the beryls from the Eastern Desert. Aluminium in the octahedral sites is also partly substituted by Cr and Fe, either ferrous or ferric that is widely demonstrated by beryl from different world localities (Eidt and Schwarz, 1988; Moroz and Eliezri 1998). Partial substitution of $Na^{(c)}$ in the channel sites in Wadi Ghazala beryl is documented by the positive correlation between Al_2O_3 and Na_2O indicating the substitution $Al^{IV} = Mg^{IV} + Na^{(c)}$. Abdalla et al. (2001) stated that the octahedral substitutions of divalent and trivalent cations for octahedral Al in Wadi Ghazala beryl are negligible which is the cause that led them to classify the mineral as "normal" beryl and not as "octahedral" beryl as documented by the present study.

Bismuth minerals:

Tables 2&3 give the chemical composition of both primary and secondary Bi-minerals inside the beryl itself as determined by the electron microprobe. Bismuthinite (Bi_2S_3) is the sole primary bismuth phase in association with Ghazala beryl. The analyzed bismuthinite is

represented by some relics in the secondary bismuth minerals, namely bismutite and beyerite as indicated petrographically (Fig. 3b).

The composition of bismuthinite indicates that the range of Bi is narrow (78.97-81.31 wt%) which is typical for the mineral $Pmc2_1$ orthorhombic lattice. Cu in the structure of the analyzed bismuthinite lies in the range of 0.49-0.62 wt% which is similar to some bismuthinite from the Romanian hydrothermal vein deposits (Cook, 1998). On the other hand, the bismuthinite of Wadi Ghazala contains appreciable Ag (0.01-0.47 wt%) where as the content of the precious metal in the Romanian examples is often close to nil. It is evident that Ag in the bismuthinite of Wadi Ghazala replaces Pb which is indicated by analyses No. 9&10 (Table 2). With respect to other precious metals, the studied bismuthinite also contain considerable gold up to 0.11 wt%.

On the basis of their chemical composition, two species of secondary Bi-minerals from the beryliferous zone at Wadi Ghazala are distinguished. The two species are carbonate gossans, namely bismutite [light canary in colour, $Bi_2(CO_3)_2O_2$] and beyerite [dark brownish yellow, $(Ca,Pb)Bi_2(CO_3)_2O_2$] that often occur in the form of colloform interlayered lamellae. The chemical composition of the analyzed bismutite-beyerite along a chemical profile in a mineral aggregate showing colloform texture, as well other aggregates that

lack colloform texture is given (Fig. 3c, Table 3). Bismutite is more enriched in Bi than beyerite containing up to 74.86 wt% and 57.98 wt%, respectively. Beyerite contains CaO in the range of 1.23-2.87 wt%.

Micas:

The electron microprobe analyses of these micas (Table 4) show the mineral trioctahedral character that classifies most of them as a transitional phase between phlogopite and biotite according to the nomenclature of Rieder et al. (1998). Plotting the analytical data of the dark brown micas at the beryl occurrence of Wadi Ghazala also supports such nomenclature (Fig. 5a). The figure also indicates considerable ionic substitution between Fe^{2+} and Mg that is slightly higher than the case of phlogopite in association with the beryls of the Eastern Desert. A wide range of ionic substitution indicated by data plots parallel to the phlogopite-eastonite solid solution line (Fig. 4a). Some analyses show that the relative enrichment in MgO and SiO_2 is accompanied by a relative depletion in TiO_2 and Al_2O_3 that suggests another type of ionic substitution, namely $Mg^{IV} + 2Si^{IV} = Ti^{VI} + 2Al^{IV}$ (Robert, 1976).

There is a distinct positive correlation between Fe/Fe+Mg and Ti cations (Fig. 5b) in a similar way to phlogopites from the mafic-ultramafic rocks worldwide (Brod et al. 2001). TiO_2 in the beryl of

Wadi Ghazala never exceeds 2.07 wt%, which is lower than that in the phlogopite of high-grade metamorphic terrains (2.80-4.00 wt%, Mohan et al. 1996) and also the phlogopite in highly evolved igneous rocks (up to 3.69 wt%, Brod et al. 2001). The wider TiO_2 range in the phlogopite-biotite of Wadi Ghazala (0.33-2.07 wt%) indicates fluctuations in the oxygen fugacity and the influx of Ti in the mineralizing fluid along the contact between the amphibolite host and the pegmatites. Also, the amphibolite contributes to the trace element compositions of the investigated micas that contain up to 0.43 wt% Cr_2O_3 and up to 0.15 wt% NiO.

Amphiboles:

Some representative electron microprobe analyses of the amphiboles from the amphibolite host at the occurrence of Wadi Ghazala (Table 5) support their petrographic nomenclature as actinolitic hornblende to hornblende (Fig. 6a). The analyzed amphiboles contain lower Al^{IV} in comparison to the tschermakite and tschermakitic hornblende in the amphibolites of the Eastern Desert (Surour, 1995).

In order to elucidate the metamorphic *P-T* conditions during the crystallization of the amphibole, some diagrams were constructed. Figure 6b shows that the studied hornblende was formed under the conditions of medium-pressure on the basis of its relative Al^{IV} and K

abundances suggested by Hynes (1982). As to temperature, metamorphic conditions corresponding to the biotite zone in the Barrovian sequences are obtained tentatively (Fig. 6c). Using the single hornblende geothermometer of Ernst and Liu (1998), a temperature range of 353-416 °C is calculated for the majority of the vailable analyses. Two rim analyses show remarkable depletion in Al^{IV} (0.35-0.46 a.u.f) and the cations of Fe (1.02-1.08) indicating temperature lowering (184-242 °C) that suggests an event of retrograde metamorphism. Such event was most probably contemporaneous to the injection of volatile-rich fluids from which beryl crystallized inside the shear zone.

Plagiocalse:

Table 5 shows that plagioclase in the amphibolite is oligoclase (An_{15-20} Ab_{75-80}). A relatively high orthoclase component, displayed by one analysis (5.53 mole%), is attributed to occasional sericitization. Due to the alteration of plagioclase and the absence of crystals in equilibrium with the amphiboles, the application of the plagioclase-hornblende geothermometer of Blundy and Holland (1990) was not possible. Plagioclase in the syenogranite is albite with the composition of An7.56-7.86 Ab90.48-90.05.

Fluid Inclusions In Beryl

The investigation of some doubly-polished wafers of Wadi Ghazala beryl revealed several populations of fluid inclusions; primary and secondary. Because the younger generation of beryl (II) is extremely fine, it was difficult to prepare sections for the fluid inclusion study. In the beryl (I), inclusions are in most cases small (20-45 μm) but some few larger inclusions, up to 75 μm, were also observed. Primary inclusions are oriented along the crystal growth zones especially in the intermediate cores and the outermost peripheral zones. On the other hand, all of the secondary inclusions are confined to healing fractures. Regardless the type of inclusions, all of them are represented by two-phase inclusions showing high degree of liquid filling (60-90 %). Morphologically, the primary inclusions are either tabular in shape (Fig. 7a) or they show oval-shaped outlines and negative crystals in very few cases. Some of the primary inclusions show amorphous necked-down appearance similar to the fluid inclusions reported by Vapnik and Moroz (2002) in the beryls from Mozambique. The secondary inclusions occur as fine elliptical or circular bodies with relative enrichment in the vapor phase.

Results of the microthermometric measurements are given in Table 6. During the freezing-heating runs, most of the two-phase primary inclusions show the formation of calthrate indicating considerable CO_2 in the vapor phase of these inclusions. It is clear that

the complete absence of any daughter crystals of halite or other phases of brine nature gives the indication that the beryl of Wadi Ghazala crystallized from low-salinity fluids. Calculation of fluid salinity using the final temperature of ice melting shows that the salinity is extremely low, in the range of 1.37-2.57 wt% $NaCl_{eq}$. This indicates extensive incorporation of meteoric water into the studied beryliferous zone (i.e. dilution) even though the original hypogene fluids were NaCl brines. Salinity of the fluid inclusions in Wadi Ghazala beryl represents the lowest range in natural beryls in comparison with other world examples. The closest salinity (3.2- 4.1 wt% $NaCl_{eq.}$) was measured in the morganite and aquamarine from the pegmatites of NE Brazil (Beurlen et al. 2001) as well as some of the Canadian emeralds (Marshall et al. 2001). Salinity of the fluid inclusions in the Afghani emeralds from Panjsher is high (20-30 wt% $NaCl_{eq.}$) and it measures as high as 80-90 wt% $NaCl_{eq.}$ in the halite saturated inclusions as given by Vapnik and Moroz (2001). The Egyptian beryls and emeralds from the "schist-type" deposits in the Eastern Desert contain fluid inclusions characterized by much higher salinity (8-22 wt% $NaCl_{eq.}$, Abdalla and Mohamed 1999) than the case of Wadi Ghazala beryl.

Homogenization temperature (T_h) of the primary inclusions in Wadi Ghazala beryl lies in the range of 226- 265 °C (Table 6). This range is lower than that of beryls from other world deposits, for example the emeralds from the pegmatites of NW Spain and Tanzania

that contain primary inclusions characterized by T_h up to 381 °C and 470 °C (Fuertes-Fuente et al. 2000; Moroz et al. 2001, respectively) or even the beryls from the "schist-type" deposits in the Eastern Desert of Egypt, 320-382 °C (El-Dougdoug et al. 1997; Abdalla and Mohamed 1999). On the other hand, much higher homogenization temperature (up to 480 °C) characterizes the primary inclusions in the beryls from the stanniferous specialized granites in the Eastern Desert (El-Shatoury et al. 1974; Abdalla and Mohamed 1999). The graphic presentation of T_h versus salinity of the investigated inclusions in Wadi Ghazala beryl shows a relatively wider salinity range of the secondary inclusions (Fig. 7b). This relation also shows the clustering of the primary and the secondary inclusions in two distinctive fields suggesting formation during two discontinuous hydrothermal stages during which the trapping of inclusions from the circulating aqueous fluids took place. As deduced from the homogenizaton temperature of both types of inclusions, the growth of beryl during the two stages was in the range of 226-265 °C and 174-187 °C, respectively. Such temperatures are very characteristic of hydrothermal systems and can not be accepted for metamorphic terrains that might have suffered migmatization .

Is Bismuth Related To Migmatization ?

In spite of its rarity in nature, one hundred and forty-three species of Bi-minerals are reported in terrestrial rocks (Lueth, 1999). The chemical properties of bismuth are very similar to those of Sb and As that classifies that metal as chalcophile element according to Goldschmidt's classification (Hale, 1981). Sulphide-bearing meteorites contain the highest Bi abundance among all the naturally occurring materials.

Careful review on the occurrence of bismuth minerals in the earth's crust revealed that these minerals are restricted in most cases to hydrothermal granitic pegmatites. Much lesser occurrences are known from the Mo-Cu porphyry-type mineralization (Peng et al., 1998) and W-skarn deposits (Carlson, 2002). No evidence for the formation of bismuth minerals during progressive high-grade regional metamorphism is obtained from the condensed survey of literature, especially those concern with migmatized terrains.

Because of its relative enrichment in the hydrothermal stage, bismuth is commonly associated with the beryl deposits of New Mexico and British Columbia (Spilde, 1999, Mihalynuk and Heaman, 2002). Bismuth minerals also associate some other ores in quartz veins and pegmatites, e.g. the tantalite and Hf-rich zircon of Argentina (Galliski et al., 2001), in addition to the uranium and REE

mineralization of Slovakia (Rojkovic et al., 1997). Maloof et al. (2001) stated that bismuth is a good pathfinder for gold and other precious metals. In this respect, bismuth minerals are recorded in the world's largest silver deposit in Bolivia (Cunningham et al., 1996).

Implication Of Bismuth On The Genesis Of Wadi Ghazala Beryl

Based on the characteristics of Wadi Ghazala bismuth-beryllium mineralization, the studied mineral assemblages and the thermometric consideration, the studied ores are typical of hydrothermal systems. The range of homogenization temperature of the primary fluid inclusions in Wadi Ghazala beryl (226-265 °C) is consistent with some world examples of bismuth mineralization. On the basis of the sulphide isotopic analysis, Lee et al. (1998) determined a temperature range of 245-315 °C for bismutinite-bearing assemblages is some Korean hydrothermal ores. A similar hydrothermal temperature range (235-245 °C) is reported by Klemm and Kräutner (2000) for the Zimbabwean gold-bismuthinite assemblages. A relatively higher temperature range (300-350 °C) was given by (Skirrow, 2000) for some hydrothermal Au-Cu-Bi in some shear-hosted hydrothermal deposits.

From the genetic point of view, it is here evident that the bismuthinite of wadi Ghazala beryliferous pegmatites is later in the

paragenitic sequence than the beryl because the bismuthinite is always found in vugs inside the beryl. Accordingly, it is evident that the primary Bi-mineral (bismuthinite) crystallized at temperature ≤ 174-265 °C. The most applicable genetic model for the studied Bi-Be mineralization can be explained in terms of ascending acidic hydrothermal fluids (rich in carbonic and nitrogenous compounds) along faults within the local shear zone at temperature lower than those obtained from the fluid inclusions in beryl. The influence of the descending meteoric water was represented by lowering the fluid temperature and salinity dilution. Lefebure (1996) estimated a temperature range of 150-250 °C for ascending hydrothermal fluids which have been derived from late-stage differentiation of acidic magmas, that later deposited bismuthinite. As a result of weathering by fluids containing dissolved carbonic gases, secondary Bi-carbonates (bismutite and beyerite) displayed psedumorphic replacement for the primary Bi-sulphide (bismuthinite).

Conclusions

The field observations at Wadi Ghazala, combined with textural characteristics, mineral chemistry and fluid inclusions data, all are not in favour of beryl crystallization in leucosomes during migmatization as concluded by Abdalla et al. (2001). In the following, the criteria that assign a hydrothermal origin for the studied beryl from Sinai are given.

1. On the basis of field relationships, the beryl at the occurrence of Wadi Ghazala occurs in pegmatites and quartz veins delineating a small-scale NNW-SSW shear zone with evidence of fluid injection and circulation in contact with the country rocks (amphibolite and within-plate granites).
2. The ore assemblage in the pegmatites is typical of hydrothermal systems being represented by beryl-fluorite-bismuth minerals-columbite arranged according to their abundances in the studied paragenesis. Fluorite and bismuth minerals demonstrate some hydrothermal ore textures such as comb-structure and crystallization as vug fillings, respectively.
3. The amphibolite host rock shows partial transformation into a dark mica rock as a result of K-metasomatism induced by the pegmatites along the contacts. Introduction of idiomorphic magnetite to the metasomatized domain of the amphibolite, in addition to the presence of apatite and metamict zircon in the micas, are all evidence of a hydrothermal signature. Presence of phlogopite-biotite inclusions in the beryl precludes any segregation of the former as melanosomes.
4. In analogy to the beryl from the contact between the ultramafic rocks and within-plate granites in the Eastern Desert, the electron microprobe analyses of Wadi Ghazala beryl show distinct ionic

substitutional trends due to partial replacement of octahedral Al by divalent and trivalent cations. The dark micas associated with the beryl at Wadi Ghazala contain TiO_2 ≤2.07 wt%, which is lower than the case of phlogopite of high grade-metamorphic terrains.

5. A retrograde metamorphic event for the amphibolite host at 184-242 °C is indicated by the geothermometry of some amphibole rims, most probably contemporaneous to the formation of beryl in the shear zone. Almost the same range of temperature is obtained from the homogenization temperature of both primary and secondary inclusions in the beryl itself (226-265 °C and 174-187 °C, respectively). Salinity of these inclusions as low as 1.37 wt% $NaCl_{eq.}$ is very peculiar in comparison with many of the world examples. Such extremely low salinity is a strong evidence of mixing of the ascending hypogene fluids with meteoric waters.
6. Despite of its similar hydrothermal origin with many of the beryls from the Eastern Desert, the beryl of Wadi Ghazala can not be affiliated to the so-called "schist-type" deposits. At the occurrence of Wadi Ghazala, neither pelitic schists nor ultramafic schistose rocks are present, and simply the hydrothermal fluids were circulating along the contact between the pegmatites and the amphibolite host rock. Injection of the hydrothermal fluid followed shearing that was responsible for the schistose-like appearance of the amphibolites and the gneissose fabrics in the granite, as we get closer to the beryliferous shear zone.

7. The absence of native bismuth at the beryl occurrence of Wadi Ghazala is in accord with high f S2 of the hydrothermal fluids. Crystallization of primary Bi-sulphides in nature indicates sulphur fugacity (-log f S2) in the range of 10-13 bar as given by Lee et al. (1998).
8. Finally, the secondary yellow to brownish yellow secondary bismuth carbonates (bismutite and beyerite) are products of weathering. Spilde (1999) confirmed the occurrence of such gossan minerals in association with beryl in the pegmatites at the Harding Mine, New Mexico, U.S.A.

Acknowledgements

Part of the laboratory work was carried out in Denmark during the stay of the author at the University of Copenhagen on a CIRIUS scientific scholarship funded by the Danish Minstery of Education. Deep thanks to Dr. Jørn Rønsbo and Mrs. Berit Winzell for the electron microprobe facility and to Mr. Ole Bang Berthelsen for scanning the plates of petrography. Dr. Ali El-Mowafy kindly guided some of the field works.

References

Abdalla H.M. and Mohamed F.H., 1999, Mineralogical and geochemical investigation of emerald and beryl mineralisation,

Pan-African Belt of Egypt: genetic and exploration aspects. J. Afr. Earth Sci., v.28: pp. 581-598.

Abdalla, H.M., El-Sayed, A.A. and El-Afandy, A.H., 2001, Geochemical and mineralogical investigation of Wadi Ghazala beryl occurrence, SE Sinai, Egypt: an example of abyssal Be-pegmatites. Egypt. J. Geol., v.45: pp. 151-168.

Aurisicchio, C., Fioravanti, G., Grubessi, O. and Zanazzi, P., 1988, Reappraisal of the crystal chemistry of beryl. Am. Mineral., v.73: pp. 826-837.

Beurlen, H., da Silva, M.R.R. and de Castro, C., 2001, Fluid inclusion microthermometry in Be-Ta-(Li-Sn)–bearing pegmatites from the Borborema Province, Northeast Brazil. Chem. Geol., v.173: pp. 107-123.

Blundy, J.D. and Holland, T.J.B., 1990, Calcic amphibole equilibria and a new amphibole-plagioclase geothermometer. Contrib. Minel. Petrol., v.104: pp. 208-224.

Bodnar, R.J. and Vityk M.O., 1994, Interpretation of microthermometric data for H_2O-NaCl fluid inclusions. In: B. De Vivo and M.L. Frezzotti (eds.), Application of Thermobarogeochemical Methods for Prospecting and Study of Ore Deposits. Verginia Tech., U.S.A.: pp. 117-130.

Bowersox, G., Snee, L.W., Foord, E.E. and Seal, R.R. II, 1991, Emeralds of the Panjshir Valley, Afghanistan. Gems Gemol., v.27: pp. 26-39.

Brod, J.A., Gaspar, J.C., de Araujo, D.P., Gibson, S.A., Thompson, R.N. and Junqueira-Brod, T.C., 2001, Phlogopite and tetra-ferriphlogopite from Brazilian carbonatite complexes: petrogenetic constraints and implications for mineral-chemistry systematics. J. Asian Earth Sci., v.19: pp. 265-296.

Carlson, G.G., 2002, Geology, mineralization and sampling results from the Kalzas tungsten property, central Yukon. In: D.S. Emond, L.H. Weston and L.L. Lewis (eds.),Yukon Exploration and Geology 2001, Exploration and Geology Services Division, Yukon Region, Indian and Northern Affairs Canada: pp. 269-278.

Cook, N.J., 1998, Bismuth sulphosalts from hydrothermal vein deposits of Neogene age, N.W. Romania. Mitt. Österr. Miner. Ges., v.143: pp. 19-39.

Cunningham, C.G., Zartman, R.E., McKee, E.H., Rye, R.O., Naseser, C.W., Sanjines, O.V., Ericksen, G.E. and Tavera, F.V., 1996, The age and thermal history of Cerro Rico de Potosi, Bolivia. Mineral. Deposita, v.31: pp. 374-385.

Eidt, T.H.M. and Schwarz, D., 1988, Die brasilianischen Smaragde und ihre Verkommen: Carnaiba/Bahia. Zeitsch. Deutsche Gemmol. Ges., v. 37: pp. 31-47.

El-Aassy, I.E., Botros, N.H., Ibrahim, M.E., Hammd, M.S. and Hassan, M.A, 1993, A new beryl occurrence in Sinai. Egypt. Mineral., v.5: pp. 1-10.

El-Dougdoug, A., Takla, M.A., Surour, A.A., Hussein, A.A. and El-Eraky, F., 1997, Mineralogy and origin of Wadi Sikait emerald, S.E. Desert, Egypt. Proceed. of the Third Conf. on Geochemistry, Alexandria University, Egypt: pp 221-239.

El-Shatoury, H.M., Takenouchi, S. and Imai, H., 1974, Fluid inclusion studies of some beryliferous pegmatites and a Tin-Tungesten lode from Egypt. Minning Geol., v.24: pp. 307-314.

Ernst, W.G. and Liu, J., 1998, Experimental phase-equilibrium study of Al- and Ti-contents of calcic amphibole in MORB – a semiquantitative thermobarometer. Am. Mineral., v.83: pp. 952-969.

Fuertes-Fuente, M., Martin-Izard, A., Boiron, M.C. and Vinuela, J.M., 2001, P-T path and fluid evolution in the Franqueira granitic pegmatite, Central Galicia, Northwestern Spain. Can. Mineral., v.38: pp. 1163-1175.

Galliski, M.A., Márquez-Zavalía, M.F., Cooper, M.A., Černý, P. and Hawthorne, F.C., 2001, Bismotantalite from northwestern Argentina: description and crystal structure. Can. Mineral., v.39: pp. 321-329.

Hale, M., 1981, Pathfinder applications of arsenic, antimony and bismuth in geochemical exploration. J. Geochem. Explor., v.15, pp. 307-323.

Hamad, M.S., 1995, Geology of the Precambrian rocks around Ein-Furtaga, West Nuweiba, Sinai, Egypt. M. Sc. Thesis, Cairo University, Egypt, 210p.

Hassan, M.A. and El-Shatoury, H.M., 1976, Beryl occurrences in Egypt. Minning Geol., v.26, pp. 253-262.

Hawthorne, F.C. and Černý, P., 1977, The alkali-metal position in Cs-Li beryl. Can. Mineral., v.15: pp. 414-421.

Hynes, A., 1982, A comparison of amphiboles from medium- and low-pressure metabasites. Contrib. Mineral. Petrol., v.81: pp. 119-125.

Klemm, D.D. and Kräutner, H.G., 2000, Hydrothermal alteration and associated mineralization in the Freda-Rebecca gold deposits – Bindura District, Zimbabwe. Mineral. Deposita, v.35: pp. 90-108.

Laird, J. and Albee, A.L., 1981, Pressure, temperature and time indications in mafic schist: their application to reconstructing polymetamorphic history of Vermont. Am. J. Sci., v.281: pp. 127-175.

Lee, C.H., Lee, H.K. and Kim, S.J., 1998, Geochemistry and mineralization age of magnesian skarn-type iron deposits of the Janggun mine, Republic of Korea. Mineral. Deposita, v.33: pp. 379-390.

Lefebure, D.V., 1996, Five-element veins Ag-Ni-Co-As-(Bi,U) – I14. In: D.V. Lefebure and T. Höy (eds.), Selected British Columbia Mineral deposit Profiles, v.2: pp. 89-91.

Lueth, V.W., 1999, Bismuth: element and geochemistry. In: C.P. Marshall and R.W. Fairbridge (eds.), Encyclopedia of Geochemistry. Kluwer Acad. Publ., Dordrect-Boston-London: pp. 43-44.

Maloof, T.L., Baker, T. and Thompson, J.F.H., 2001, The Dublin Gulch intrusion-hosted gold deposit, Tombstone plutonic suite, Yukon Territory, Canada. Mineral. Deposita, v.36: pp. 583-593.

Marshall, D., Groat, L., Giuliani, G., Scott Ercit, T., Gault, R.A., Wise, M.A., Wengzynowski, W. and Eaton, W.D., 2001, Low salinity fluid inclusions in Canadian emeralds: The Crown Showing, southeastern Yukon, Canada. In: F. Noronha, A. Dória and A. Guedes (eds.), XVI ECROFI Current Research on Fluid Inclusions, Porto 2001, Portugal, Memorial No. 7: pp. 279-282 (Extended Abstract).

Mihalynuk, M.G. and Heaman, L.M., 2002, Age of mineralized porphyry at the Logtung deposit W-Mo-Bi-Be (beryl, aquamarine), Northwest BC. Geological Fieldwork 2001, Paper 2002-1, British Columbia Geological Survey: pp. 35-40.

Mohan, A., Prakash, D. and Motoyoshi, Y., 1996, Decompositional *P-T* history in sappharine-bearing granulites from Kodaikanal, southern India. J. Southeast Asian Earth Sci., v.14: pp. 231-243.

Moroz, I.I. and Eliezri, I.Z., 1998, Emerald chemistry from different deposits: an electron microprobe study. Austr. Gemmol., v.20: pp. 64-69.

Moroz, I.I., Vapnik, Y., Eliezri, I. and Roth, M., 2001, Mineral and fluid inclusion study of emeralds from the Lake Manyara and Sumbawanga deposits, Tanzania. J. Afr. Earth Sci., v.33: pp. 377-390.

Omar, S.A.M., 2001, Characterization and evaluation of some beryl occurrences in the Eastern Desert, Egypt. Ph. D. Thesis, Cairo University, Egypt, 260p.

Peng, Z., Watanabe, M., Hoshino, K., Sueoka, S., Yano, T. and Nishido, H., 1998, The Machangqing copper-molybdenum deposits, Yunnag, China – an example of Himalayan porphyry-hosted Cu-Mo mineralization. Mineral. Petrol., v.63: pp. 95-117.

Potter, R.W. II and Brown, D.L., 1977, The volumetric properties of aqueous sodium chloride solutions from 0 to 500 °C at pressures up to 2000 bars based on a regression of available data in the literature. U.S. Geol. Surv. Bull. 1421-C: 1-36.

Rieder, M., Cavazzini, G., D'Yakonov, Y.S., Frank-Kamenetskii, V.A., Gottardi, G., Giggenheim, S., Koval, P.V., Muller, G., Neiva, A.M.R., Radoslovich, E.W., Robert, J.-L., Sassi, F.P., Takeda, H., Weiss, Z. and Wones, D.R., 1998, Nomenclature of the micas. Can. Mineral., v.36: pp. 905-912.

Rojkovic, I., Haber, M. and Novotny, L., 1997, U-Au-Co-Bi-REE mineralization in the Gemeric Unit (Western Carpathians, Slovakia). Geol. Carpathica, v.48: pp. 303-313.

Robert, J.-L., 1976, Titanium solubility in synthetic phlogopite solid solutions. Chem. Geol., v.17: pp. 213-227.

Skirrow, R.G., 2000, Gold-copper-bismuth deposits of the Tennant Creek District, Australia: a reappraisal of diverse high-grade systems. In: T.M. Porter (ed.), Hydrothermal Iron Oxide Copper-Gold and Related Deposits: A Global Perspective, v.1, Austr. Mineral Found., Adelaide, 350p.

Spilde, M.N., 1999, Bismuth minerals from the Harding Mine: more than just yellow-green grunge. New Mexico Geology, v.21: pp. 15-18.

Surour, A.A., 1993, Petrology, geochemistry and mineralization of some ultramafic rocks, Egypt. Ph. D. Thesis, Cairo University.

Surour, A.A., 1995, Medium- to high-pressure garnet amphibolites from Gebel Zabara and Wadi Sikait, south Eastern Desert, Egypt. J. Afr. Earth Sci., v.21: pp. 443-457.

Takla, M.A., Surour, A.A., Hassan, M.A. and Omar, S.A., 2002, Source of beryllium, genesis and evaluation of some beryl occurrences in the Eastern Desert of Egypt. J. Afr. Earth Sci. (in press).

Vapnik, Ye and Moroz., I., 2001, Fluid inclusions in Panjshir emerald (Afghanistan). In: F. Noronha, A. Dória and A. Guedes (eds.),

XVI ECROFI Current Research on Fluid Inclusions, Porto 2001, Portugal, Memorial No. 7: pp 451-454.

Vapnik, Ye and Moroz, I., 2002, Compositions and formation conditions of fluid inclusions in emerald from the Maria deposit (Mozambique). Mineral. Mag., v.66: 201-213.

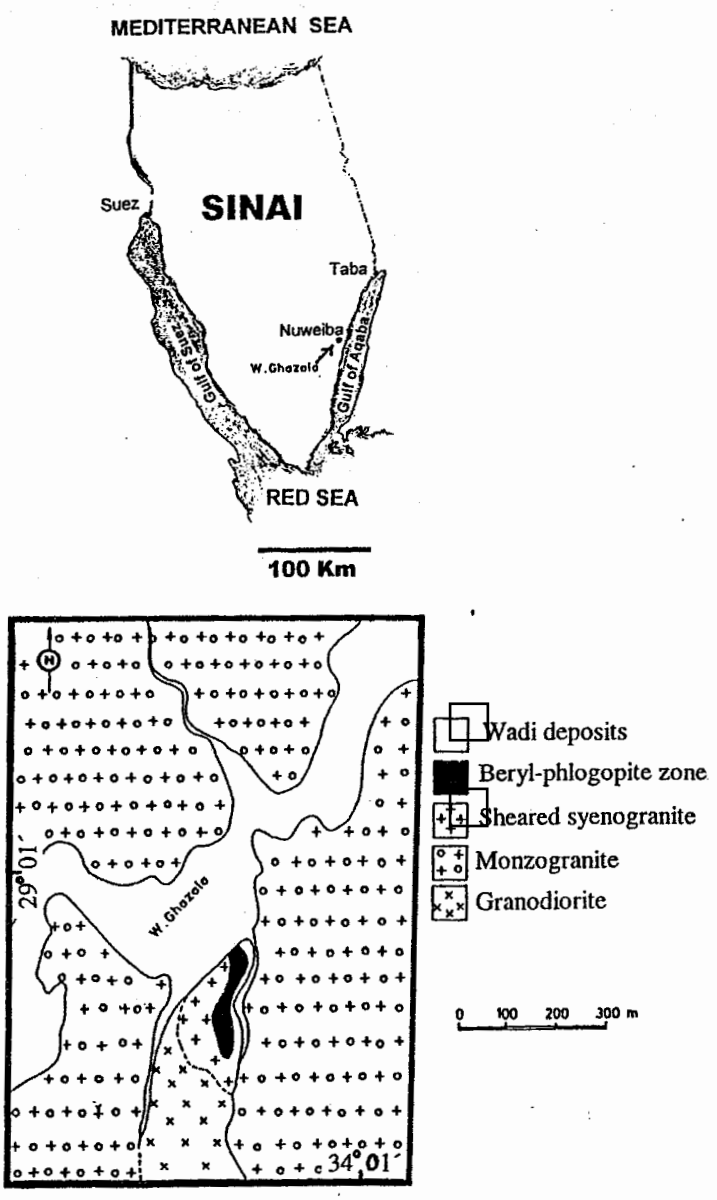

Fig. 1: Simplified geological map of Wadi Ghazala beryl occurrence (Modified after El-Aassy et al., 1993; Hamad, 1995).

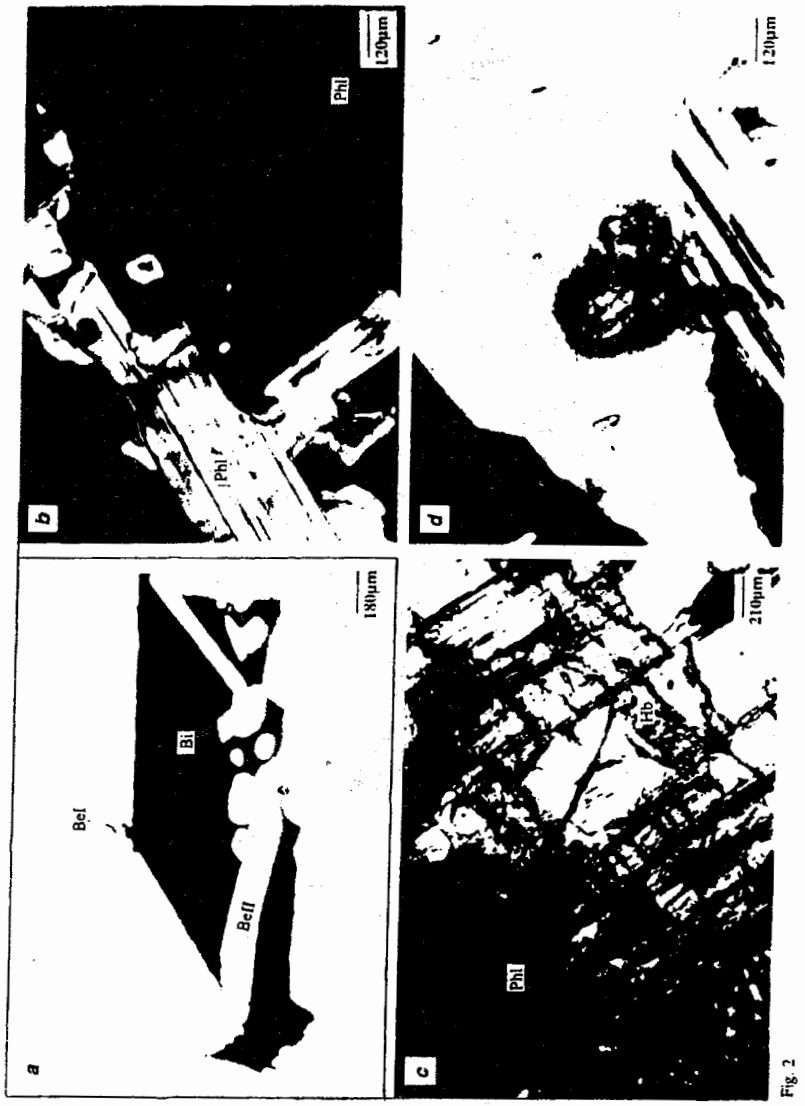

Fig. 2: Petrography of the beryl-bearing rocks:
a) Coarse beryl (Be I) hosting a finer generation of beryl (Be II) and bismuth minerals (Bi) in vugs, pegmatite, PPL. b) Corrosion of coarse beryl (dark) by phlogopite flakes (Phl). The former also contains inclusions of the latter, pegmatite, C.N. c) Partial transformation of hornblende (Hb) into phlogopite (Phl), metasomatized amphibolite, P.P.L. d) Coarse and fine inclusions of metamict zircon in phlogopite, pegmatite, C.N.

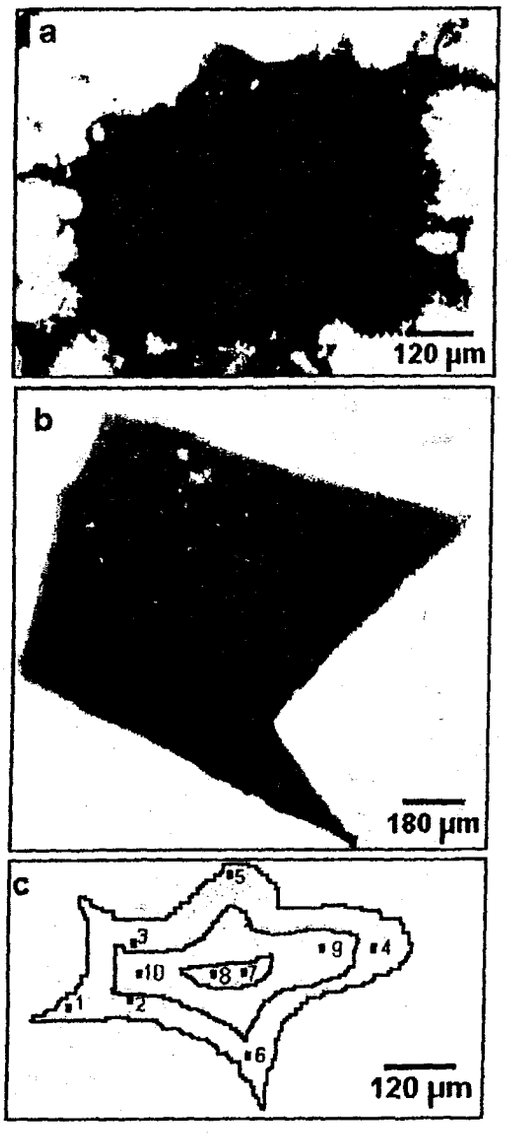

Fig. 3: a) Columbite grain showing lighter periphery due to metamictization
b) Relict bismuthinite (black at the center) in a mixture of bismutite and beyerite
c) Sketch for collform bismutite- beyerite showing alternation of both minerals
and the numbers of the electron microprobe spot analyses given in Table 5.

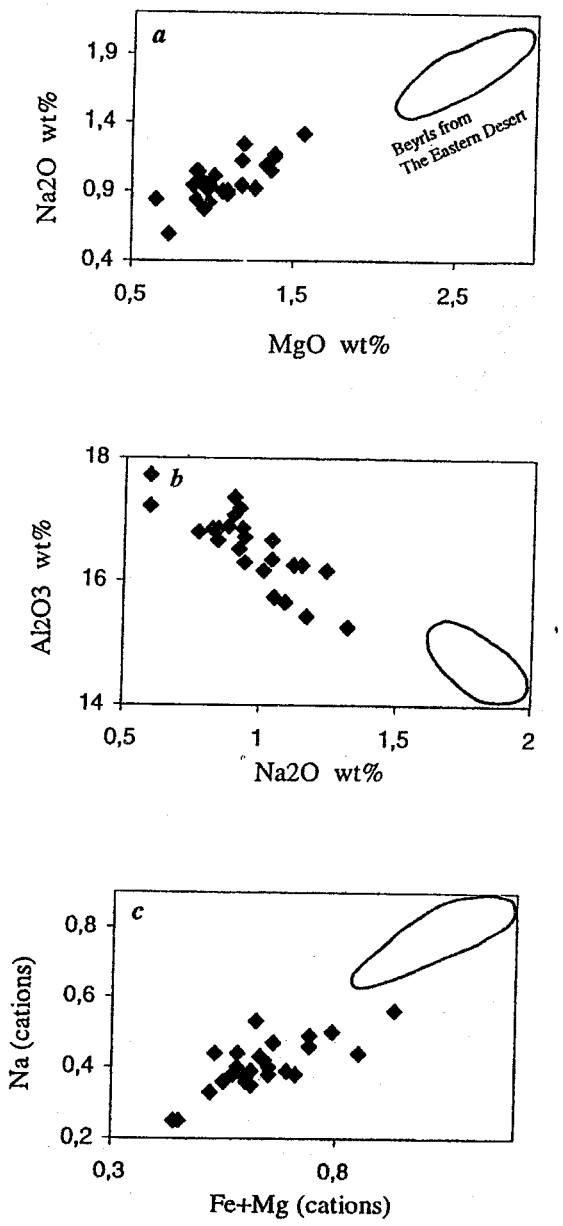

Fig. 4: Different types of substitutions of octahedral Al in Wadi Ghazala beryl as indicated by the binary relations:
a) MgO vs. Na_2O

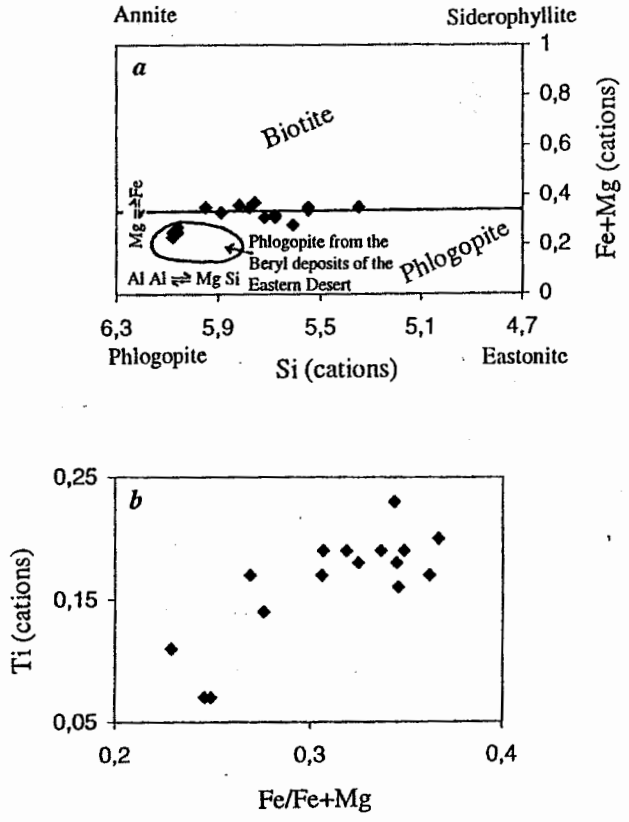

Fig. 5: a. Transitional nature of Wadi Ghazala micas from phlogopite to biotite. The field of phlogopite from the Eastern Desert of Egypt is defined by the data cited in Surour (1993); El-Dougdoug et al. (1997); Abdalla and Mohamed (1999). b. Positive correlation between Fe/Fe+Mg and Ti in Wadi Ghazala micas.

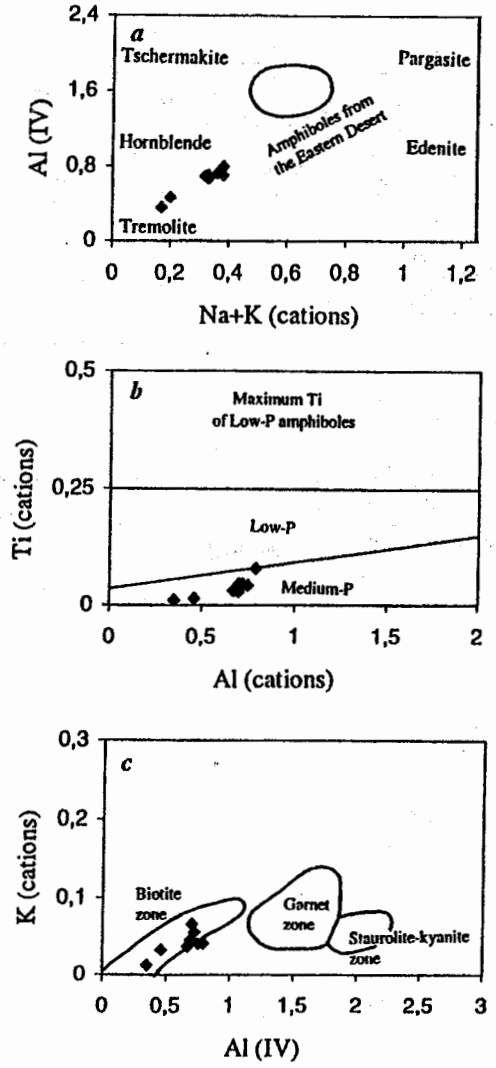

Fig. 6: a. Composition of amphiboles in the amphibolite of Wadi Ghazala. The field of amphiboles in the amphibolites from the Eastern Desert is defined by Surour (1995).
b. Medium-preassure characteristics of the studied amphiboles using the digram of Hynes (1982).
c. Formation of the studied amphiboles in conditions corresponding to the biotite zone in the Barrovian sequences. The fields of different zones are fit by Laird and Albee (1981).

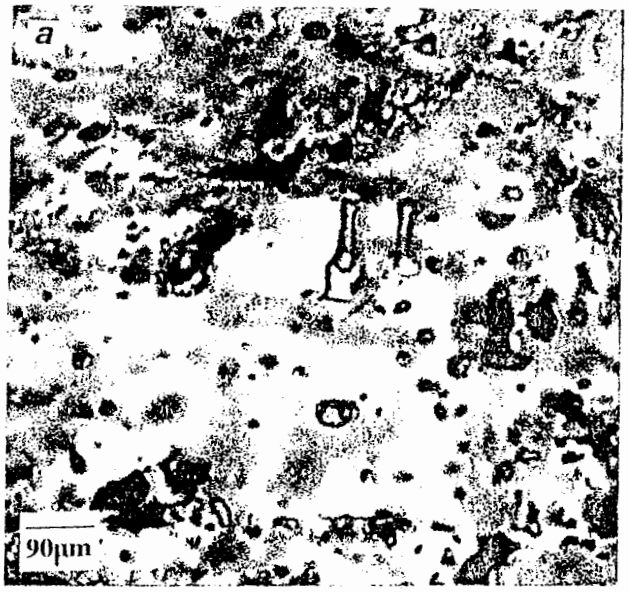

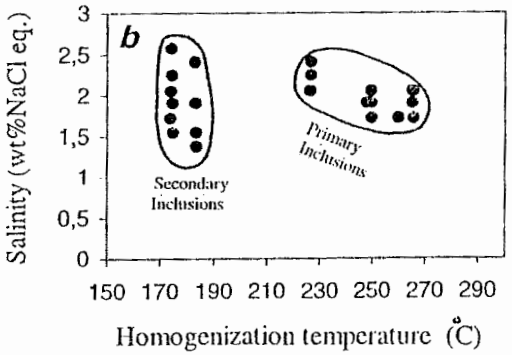

Fig. 7: a: Primary fluid inclusions in Wadi Ghazala beryl
b. Clustering of the primary and secondary inclusions in the beryl by the plot of their homogenization temperature vs. salinity

Table 1: Electron microprobe analyses of Wadi Ghazala beryl

	67	68	70	71	131	132	133	54	55	56	72	73	40	41	42	43	44	46	54	47	48	49	50	51
Oxides wt%	R	C	C	R	R	C	R	R	C	C	R	R	R	R	IC	C	IC	R	C	R	IC	C	IC	R
SiO2	65.21	64.46	65.38	65.66	65.23	65.34	64.5	64.54	64.63	65.12	65.06	65.64	65.36	64.63	65.04	65.98	64.95	65.04	65.08	65.31	64.39	65.38	64.03	64.57
TiO2	0.01	0.01	0.01	0.01	0.01	0.01	0.01	0.01	0.01	0.01	0.01	0.01	0.01	0.01	0.01	0.01	0.01	0.01	0.01	0.01	0.01	0.01	0.01	0.01
Al2O3	16.34	16.25	16.65	16.84	17.18	17.36	16.25	16.16	16.16	16.87	16.85	16.65	16.70	16.51	17.21	17.72	16.78	15.65	17.06	15.73	15.42	16.78	16.21	15.26
Cr2O3	0.01	0.13	0.07	0.05	0.02	0.01	0.07	0.02	0.01	0.01	0.02	0.07	0.07	0.01	0.01	0.01	0.01	0.01	0.01	0.01	0.01	0.05	0.01	0.01
FeO*	1.57	1.54	1.31	1.61	1.48	1.25	1.61	1.29	1.63	1.35	1.61	1.43	1.51	1.52	1.17	1.11	1.17	1.72	1.69	2.24	1.85	1.78	1.99	2.32
MgO	0.90	1.18	0.91	0.65	0.96	1.06	1.38	1.19	1.01	1.09	0.99	0.90	1.18	1.26	0.73	0.73	0.95	1.33	1.06	1.36	1.38	0.93	1.09	1.56
CaO	0.01	0.01	0.01	0.01	0.01	0.01	0.01	0.01	0.01	0.01	0.08	0.11	0.07	0.01	0.01	0.01	0.01	0.01	0.07	0.01	0.14	0.01	0.01	0.01
MnO	0.20	0.01	0.20	0.01	0.01	0.01	0.01	0.01	0.01	0.01	0.01	0.01	0.01	0.01	0.01	0.01	0.01	0.23	0.01	0.01	0.01	0.01	0.01	0.22
Na2O	1.04	1.12	1.04	0.84	0.92	0.90	1.15	1.24	1.01	0.88	0.93	0.84	0.94	0.92	0.59	0.59	0.77	1.09	0.90	1.05	1.17	0.98	0.90	1.32
K2O	0.01	0.01	0.13	0.01	0.01	0.14	0.07	0.01	0.01	0.01	0.17	0.07	0.01	0.14	0.10	0.01	0.17	0.18	0.14	0.27	0.27	0.15	0.24	0.26
NiO	0.01	0.05	0.04	0.01	0.01	0.01	0.05	0.06	0.01	0.05	0.01	0.04	0.07	0.01	0.01	0.01	0.01	0.07	0.01	0.06	0.01	0.01	0.01	0.01
Total	85.31	84.77	85.75	85.70	85.84	86.10	85.19	84.54	84.50	85.41	85.74	85.77	85.93	85.03	84.89	86.19	84.84	85.34	86.04	86.06	84.86	86.09	84.51	85.55
Structural formula on the basis of 36 oxygen atoms																								
Si	12.21	14.04	14.24	14.30	14.21	14.23	14.07	14.06	14.08	14.19	14.17	14.30	14.24	14.08	14.87	14.57	14.15	14.17	14.18	14.23	14.03	14.24	13.95	14.07
Ti	0.0017	0.0017	0.0017	0.0017	0.0017	0.0017	0.0017	0.0017	0.0017	0.0017	0.0017	0.0017	0.0017	0.0017	0.0017	0.0017	0.0017	0.0017	0.0017	0.0017	0.0017	0.0017	0.0017	0.0017
Al	4.23	4.21	4.31	4.36	4.45	4.50	4.21	4.19	4.19	4.37	3.36	4.31	4.33	4.28	4.46	4.59	4.35	4.05	4.42	4.07	3.99	4.35	4.20	3.95
Cr	0.0007	0.0020	0.0180	0.0084	0.0034	0.0017	0.0180	0.0034	0.0017	0.0017	0.0034	0.0180	0.0012	0.0017	0.0017	0.0017	0.0017	0.0017	0.0017	0.0017	0.0017	0.0084	0.0017	0.0017
Fe	0.29	0.28	0.24	0.29	0.27	0.23	0.29	0.23	0.30	0.25	0.29	0.26	0.27	0.28	0.21	0.20	0.21	0.31	0.31	0.41	0.34	0.34	0.36	0.42
Mg	0.29	0.38	0.29	0.21	0.31	0.34	0.45	0.39	0.33	0.35	0.32	0.29	0.38	0.41	0.24	0.24	0.31	0.43	0.34	0.44	0.45	0.30	0.35	0.51
Ca	0.0023	0.0023	0.0023	0.0023	0.0023	0.0023	0.0023	0.0023	0.0023	0.0023	0.0186	0.0255	0.0162	0.0023	0.0023	0.0023	0.0023	0.0023	0.0162	0.0023	0.0325	0.0023	0.0023	0.0023
Mn	0.040	0.002	0.040	0.002	0.002	0.002	0.002	0.002	0.002	0.002	0.002	0.002	0.002	0.002	0.002	0.002	0.002	0.046	0.002	0.002	0.002	0.002	0.002	0.044
Na	0.44	0.47	0.44	0.36	0.39	0.38	0.49	0.53	0.43	0.37	0.39	0.36	0.40	0.39	0.25	0.25	0.35	0.46	0.38	0.44	0.50	0.42	0.38	0.56
K	0.003	0.003	0.039	0.003	0.003	0.39	0.019	0.003	0.003	0.005	0.019	0.003	0.003	0.039	0.003	0.003	0.047	0.047	0.039	0.075	0.075	0.041	0.066	0.075
Ni	0.0016	0.0078	0.0062	0.0016	0.0016	0.0016	0.0078	0.0093	0.0016	0.0078	0.0016	0.0062	0.0109	0.0016	0.0016	0.0016	0.0010	0.0109	0.0016	0.0093	0.0016	0.0016	0.0016	0.0016
Fe+Mg	0.58	0.66	0.53	0.60	0.58	0.57	0.74	0.62	0.63	0.60	0.61	0.55	0.65	0.69	0.45	0.44	0.52	0.74	0.65	0.85	0.79	0.64	0.71	0.93

C: core IC: inner core R: rim

Table 2: Electron microprobe analyses of bismuth sulphide (bismuthinite)

Analysis No.	1	2	3	4	5	6	7	8	9	10
Element (wt%)										
S	19.05	18.73	19.20	19.33	18.78	19.32	19.10	19.43	19.07	19.31
Fe	0.01	0.01	0.01	0.01	0.01	0.04	0.03	0.05	0.01	0.01
Cu	0.50	0.55	0.58	0.62	0.56	0.61	0.59	0.54	0.49	0.54
As	0.01	0.01	0.01	0.01	0.01	0.01	0.01	0.01	0.01	0.01
Bi	78.97	79.53	81.31	80.58	81.28	81.13	80.56	80.61	80.61	80.42
Pb	1.97	1.68	0.01	0.01	0.30	0.28	0.01	0.01	0.47	0.01
Ag	0.01	0.01	0.01	0.05	0.14	0.11	0.33	0.01	0.01	0.49
Au	0.01	0.04	0.09	0.01	0.11	0.01	0.07	0.02	0.01	0.01
------	-------	-------	-------	-------	-------	-------	-------	-------	-------	-------
Total	100.53	100.56	101.22	100.62	101.19	101.51	100.70	100.68	100.68	100.80

Table 3: Electron microprobe analyses of bismuth carbonates (bismutite and beyerite)

Mineral	Bismutite								Beyerite	
Analysis No.	1	2	3	4	5	6	7	8	9	10
Element (wt%)										
S	0.24	0.25	0.05	0.33	0.08	0.01	0.01	0.43	0.43	0.01
Fe	0.01	0.01	0.01	0.01	0.02	0.02	0.26	0.01	0.10	0.08
Cu	0.22	0.17	0.37	0.07	0.21	0.18	0.18	0.13	0.13	0.22
As	0.01	0.01	0.01	0.01	0.01	0.01	0.01	0.01	0.01	0.01
Bi	71.40	71.56	72.48	74.86	70.10	65.15	62.35	57.81	57.81	57.98
Pb	2.37	2.01	1.00	0.99	0.43	0.14	0.41	1.13	1.13	0.17
Ag	0.37	0.16	0.01	0.29	0.16	0.01	0.01	0.50	0.50	0.01
Au	0.01	0.01	0.01	0.07	0.08	0.13	0.01	0.01	0.01	0.01
------	-------	-------	-------	-------	-------	-------	-------	-------	-------	-------
Total	74.63	74.18	73.94	76.63	71.09	65.65	63.24	60.12	60.12	58.49
CaO (wt%)									1.23	2.87

Table 4: Electron microprobe analyses of the dark micas (biotite-phlogopite)

	60	61	63	64	65	66	129	130	134	136	138	60	63	64	67
Oxides wt%															
SiO2	40.39	39.26	39.98	37.70	39.51	39.13	41.16	38.10	41.31	41.29	41.18	38.83	38.55	38.55	37.72
TiO2	1.67	2.07	1.70	1.43	1.52	1.88	1.53	0.33	1.00	0.67	0.68	1.52	1.73	1.78	1.70
Al2O3	12.85	13.26	12.68	11.95	12.95	12.41	12.12	10.98	11.60	12.02	11.84	13.95	13.73	13.37	13.87
Cr2O3	0.02	0.04	0.01	0.05	0.01	0.02	0.10	0.28	0.26	0.43	0.43	0.20	0.37	0.14	0.10
FeO*	14.13	12.98	13.41	13.38	14.27	14.52	14.84	14.64	9.49	10.30	10.20	12.68	13.17	12.96	14.20
MgO	16.15	14.77	16.58	15.06	14.98	14.91	17.63	16.68	18.99	18.64	18.55	17.16	16.78	17.44	16.68
CaO	0.08	0.71	0.01	0.11	0.01	0.08	0.25	0.11	0.14	0.01	0.01	0.01	0.01	0.01	0.01
MnO	0.66	0.49	0.19	0.75	0.56	0.88	0.28	0.43	0.41	0.20	0.01	0.41	0.15	0.37	0.45
Na2O	0.17	0.11	0.04	0.20	0.08	0.11	0.13	0.19	0.21	0.19	0.21	0.07	0.08	0.07	0.13
K2O	10.07	9.65	9.87	9.40	9.98	9.70	10.34	9.09	9.73	9.93	10.13	9.84	9.48	9.84	10.01
NiO	0.08	0.11	0.06	0.11	0.07	0.01	0.10	0.10	0.14	0.05	0.08	0.15	0.10	0.04	0.15
Total	96.27	93.45	94.58	90.14	93.94	93.65	94.48	90.93	93.28	93.73	93.32	94.82	94.15	94.57	95.02
Structural formula on the basis of 22 oxygen atoms (anhydrous)															
Si	5.95	5.78	5.89	5.55	5.82	5.76	6.06	5.61	6.08	6.08	6.06	5.72	5.68	5.68	5.55
Ti	0.18	.23	0.18	0.16	0.17	0.20	0.17	0.14	0.11	0.07	0.07	0.17	0.19	0.19	0.19
Al(IV)	2.02	2.22	2.11	2.04	2.18	2.12	1.94	1.87	1.92	1.92	1.94	2.28	2.32	2.28	2.37
Al(VI)	0.14	0.04	0.05	0	0.03	0	0.13	0	0.06	0.13	0.08	0.10	0.02	0	0
Cr	0.0022	0.0046	0.0011	0.0057	0.0011	0.0022	0.0110	0.032	0.03	0.039	0.049	0.023	0.042	0.016	0.0111
Fe	1.84	1.67	1.71	1.72	1.84	1.87	1.40	1.89	1.22	1.33	1.31	1.63	1.70	1.67	1.83
Mg	3.49	3.19	3.58	3.25	3.24	3.22	3.81	3.60	4.10	4.03	4.01	3.71	3.62	3.77	3.60
Ca	0.010	0.085	0.0012	0.013	0.0012	0.010	0.03	0.013	0.017	0.0012	0.0012	0.0012	0.0012	0.0012	0.0012
Mn	0.081	0.06	0.023	0.092	0.069	0.011	0.035	0.053	0.05	0.025	0.001	0.05	0.018	0.046	0.055
Na	0.048	0.031	0.040	0.057	0.023	0.031	0.037	0.054	0.06	0.054	0.060	0.020	0.023	0.020	0.37
K	1.89	1.81	1.85	1.76	1.87	1.82	1.94	1.71	1.83	1.80	1.90	1.85	1.78	1.85	1.88
Ni	0.009	0.012	0.007	0.012	0.008	0.001	0.011	0.011	0.015	0.005	0.009	0.016	0.011	0.004	0.016
Fe+Mg	5.33	4.86	5.30	4.97	5.08	5.09	5.21	5.49	5.32	5.33	5.32	5.33	5.32	5.44	5.43
Fe/Fe+Mg	0.345	0.344	0.325	0.346	0.362	0.367	0.69	0.344	0.229	0.249	0.246	0.306	0.319	0.307	0.337

Table 5: Electron microprobe analyses of amphibole and plagioclase

	59 C	61 C	65 C	66 C	76 C	77 R	78 R	79 R	80 R	68 R	69 R	70 R	72 C	30 R	31 R
	Amphibole									Plagioclase					
Oxides wt%															
SiO2	50.68	51.28	53.38	50.47	51.62	53.08	50.92	51.30	50.72	62.90	61.42	61.38	62.66	65.64	65.64
TiO2	0.28	0.30	0.10	0.41	0.45	0.13	0.45	0.30	0.77	0.21	0.19	0.01	0.01	0.10	0.01
Al2O3	4.19	4.12	2.10	4.52	4.76	2.76	4.31	4.14	4.74	23.75	24.66	23.81	23.68	19.56	21.86
Cr2O3	0.19	0.07	0.09	0.19	0.16	0.07	0.05	0.09	0.16	n.d.	n.d.	n.d.	n.d.	n.d.	n.d.
FeO*	11.30	10.59	9.76	12.04	10.98	9.17	11.34	11.54	12.17	0.01	0.96	0.31	0.01	0.49	0.49
MgO	16.13	16.71	17.33	16.07	16.45	18.01	15.95	16.12	15.48	0.26	0.16	0.01	0.35	0.24	0.01
CaO	12.34	12.34	12.56	12.05	11.91	12.76	11.99	11.92	11.95	4.30	3.64	5.05	3.06	1.75	1.62
MnO	0.81	0.49	0.36	0.45	0.35	0.45	0.45	0.56	0.58	0.01	0.01	0.01	0.01	0.20	0.01
Na2O	0.96	1.04	0.57	1.19	1.24	0.62	1.08	1.02	1.23	9.23	8.29	8.82	9.06	11.12	10.39
K2O	0.37	0.21	0.07	0.23	0.25	0.18	0.31	0.25	0.23	0.10	1.13	0.18	0.71	0.30	0.07
NiO	0.08	0.07	0.01	0.09	0.04	0.10	0.01	0.07	0.08	n.d.	n.d.	n.d.	n.d.	n.d.	n.d.
Total	97.33	97.22	96.33	97.71	98.21	97.33	96.86	97.31	98.11	100.77	100.46	99.58	99.55	99.40	100.01
	Structural formula on the basis of 23 oxygen atoms (anhydrous)									Structural formula on the basis of 32 oxygen atoms					
Si	7.17	7.25	7.55	7.14	7.30	7.51	7.20	7.26	7.17	11.13	10.87	10.86	10.09	10.62	10.62
Ti	0.028	0.03	0.01	0.041	0.045	0.013	0.045	0.030	0.077	0.021	0.019	0.001	0.001	0.010	0.001
Al(IV)	0.70	0.67	0.35	0.75	0.70	0.46	0.72	0.69	0.79	4.95	5.14	4.96	4.93	4.08	4.55
Al(VI)	0	0	0	0	0.09	0	0	0	0						
Cr	0.020	0.008	0.010	0.020	0	0.008	0.005	0.010	0.017	n.d.	n.d.	n.d.	n.d.	n.d.	n.d.
Fe	1.26	1.18	1.08	1.34	0.017	1.02	1.26	1.28	1.35	0.002	0.20	0.065	0.002	0.102	0.102
Mg	3.39	3.52	3.65	3.38	1.22	3.79	3.36	3.39	3.26	0.071	0.044	0.003	0.096	0.066	0.003
Ca	1.87	1.87	1.90	1.83	3.46	1.93	1.82	1.81	1.81	0.814	0.689	0.956	0.579	0.331	0.307
Mn	0.098	0.059	0.044	0.055	1.80	0.055	0.055	0.68	0.070	0.002	0.002	0.002	0.002	0.003	0.002
Na	0.26	0.29	0.16	0.33	0.043	0.17	0.30	0.28	0.34	3.16	3.84	3.02	3.10	3.81	3.74
K	0.066	0.037	0.012	0.041	0.34	0.032	0.055	0.044	0.041	0.023	0.265	0.042	0.166	0.070	0.016
Ni	0.008	0.007	0.001	0.009	0.044	0.001	0.001	0.007	0.008	n.d.	n.d.	n.d.	n.d.	n.d.	n.d.
T (°C)*	369	353	184	395	369	242	379	363	Anorthite	20.35	14.37	23.79	15.06	7.86	7.56
									Albite	79.08	80.10	75.16	80.62	90.48	92.05
									Orthoclase	0.57	5.53	1.05	4.32	1.66	0.39

* Temperature is calculated according to the amphibole geothermometery of Ernst and Liu (1998)

C: core R: rim

Table 6: Microthermometric measurements of the fluid inclusions in Wadi Ghazala bery

Homogenization Temperature T_h (°C)	Eutectic Temperature T_e (°C)	Final Temperature of ice melting T_i (°C)
174.6	-32.8	-1.1
174.3 (6)*	-31.9 (6)	-1.5 (6)
174.8	-32.7	-0.9
174.1	-32.6	-1.2
173.9	-32.5	-1.0
174.7 (2)	-23.9 (2)	-1.1 (2)
174.6	-23.7	-1.1
174.5	-23.6	-1.3
183.1	-23.5	-1.4
183.2 (2)	-23.9	-1.1
183.4	-22.8	-0.9
183.6	-22.7	-0.8
183.5	-	-1.1
186.5	-	-1.1
186.9	-	-1.1
186.8	-	-1.1
186.3	-	-1.1
226.7	-	-1.3
226.8	-	-1.4
226.3	-	-1.2
226.5	-	-1.2
226.4	-	-1.2
265.3	-	-1.2
265.8	-22.8	-1.2
265.4	-22.9	-1.1
265.7	-22.7	-1.0
260.0	-22.5	-1.0
247.8 (3)	-22.4 (3)	-1.1 (3)
249.7 (2)	-22.6 (2)	-1.0 (2)
249.8 (4)	-22.7 (4)	-1.1 (4)
249.6 (3)	-23.8 (3)	-1.2 (3)
249.5 (2)	-23.9 (2)	-1.1 (2)

* Numbers between brackets indicate number of readings of this temperature.
- Eutectic temperature was not determined because the size of inclusions was extremly fine.

نشأة تمعدن البيريليوم و البيزموث بمنطقة وادي غزالة (جنوب شرق سيناء، مصر) : دلائل من كيمياء المعادن و المكتنفات السائلة

عادل عبد الله سرور

قسم الجيولوجيا- كلية العلوم- جامعة القاهرة

تستخدم الدراسة الحالية بعض الوسائل البترولوجية مثل كيمياء المعادن و المكتنفات السائلة من أجل تمييز تمعدنات البيريليوم و البيزموث بمنطقة وادي غزالة، و علي وجه الخصوص معدن البيريل واستخلاص نموذج التكوين غرض ازالة اللبس حولة حيث أن بعض الدراسات الحديثة (عبد الله و آخرون، ٢٠٠١) قد خلصت إلى ربط اصل و نشأة معدن البيريل بالمنطقة بتكون المستخلصات البيجماتيتية فاتحة اللون الناتجة عن طريق المجمتة.

توضح المشاهدات الحقلية بواسطة المؤلف الحالي وجود معدن البيريل في عروق المرو و البيجماتيت معاً، و كلاهما محددان بمنطقة قص ذات نطاق محدود داخل صخور أمفيبوليت. و تتم عملية إحلال تدريجية لصخور الأمفيبوليت بصخور ميكائية داكنة اللون بفعل التغيرات الميتاسوماتيه البوتاسية و المثبتة أيضا ببعض القرائن البتروجرافية. و بناءا علي هذه المشاهدات الحقلية و كذلك وجود محصورات من الميكا داخل البيريل نفسه، فأن نشأة البيريل في هذه الحالة لا يمكن أن يكون قد تم عن طريق تمايز الصخور المتحولة. و يدل علي ذلك أيضا أن معدن البيريل يكون مقترن بصحبة معادن حرمائية أصيلة مثل الفلوريت و الكلومبيت و بعض معادن البيزموث. كما أن دراسة التركيب الكيميائي لمعدني البيريل و الميكا عن طريق المجس الالكتروني الثاقب (الميكروبروب) توضح مميزات جلية لنظم تمعدنات المحاليل الحرمائية.

معادن البيزموث بتواجد بيريل وادي غزالة موجودة دائما في تجاويف داخل معدن البيريل نفسه بعروق البيجماتيت فقط مما يدل علي تكون زمني لاحق للبيريل. و قد أمكن التمييز بين معادن بيزموث أوليه عبارة عن كبريتيدات (بيزموثينيت) و أخري ثانوية عبارة عن نواتج تجوية مثل الكربونات المائية (بيزموتيت و بياريت).

تدل درجات حرارة تجانس المكتنفات السائلة الأولية و الثانوية الموجودة بمعدن البيريل علي حبس المحلول الحرمائي عند درجات حرارة تتراوح من ١٧٤ إلي ٢٦٥ درجة مئوية و تتميز هذه المكتنفات بملوحة متدنية تبلغ قيمتها الأقل ١,٣٧ وزن مئوي لكلوريد الصوديوم المكافئ مقارنة بالأمثلة العالمية الأخرى. وهذا يدل علي درجة امتزاج غالية مع مياه الأمطار المتوغلة من السطح إلى داخل منطقة القص و الذي أدي أيضا إلى اختفاء البلورات الملحية الصلبة بالمكتنفات السائلة المدروسة.